Analytica Chimica Acta xxx (2016) 1–7

Contents lists available at ScienceDirect

Analytica Chimica Acta

journal homepage: www.elsevier.com/locate/aca

A regenerative ratiometric electrochemical biosensor for selective detecting Hg^{2+} based on Y-shaped/hairpin DNA transformation

Jing Jia [a], Hong Guo Chen [a], Ji Feng [a], Jing Lei Lei [b], Hong Qun Luo [a, **], Nian Bing Li [a, *]

[a] Key Laboratory of Eco-environments in Three Gorges Reservoir Region (Ministry of Education), School of Chemistry and Chemical Engineering, Southwest University, Chongqing 400715, PR China
[b] School of Chemistry and Chemical Engineering, Chongqing University, Chongqing 400044, PR China

HIGHLIGHTS

- The dual-signaling ratiometric method improved the precision and sensitivity.
- The fabrication of biosensor is less time-consuming and simpler.
- The biosensor shows excellent selectivity and repeatability.
- This biosensor can be easily regenerated by using L-cysteine.

GRAPHICAL ABSTRACT

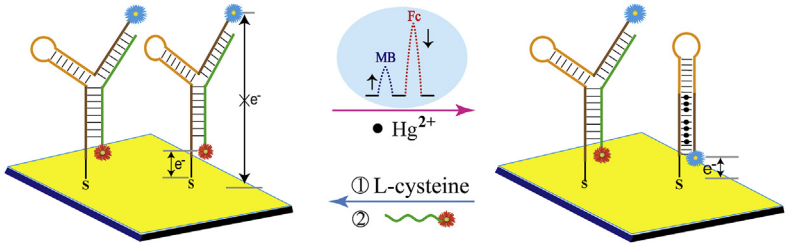

ARTICLE INFO

Article history:
Received 22 September 2015
Received in revised form
28 December 2015
Accepted 29 December 2015
Available online xxx

Keywords:
Ratiometric biosensor
Y-shaped DNA
Mercury ion
Regeneration
Square wave voltammetry

ABSTRACT

Inspired by dual-signaling ratiometric mechanism which could reduce the influence of the environmental change, a novel, convenient, and reliable method for the detection of mercury ions (Hg^{2+}) based on Y-shaped DNA (Y-DNA) was developed. Firstly, the Y-DNA was formed via the simple annealing way of using two different redox probes simultaneously, omitting the multiple operation steps on the electrode. The Y-DNA was immobilized on the gold electrode surface and then an obvious ferrocene (Fc) signal and a weak methylene blue (MB) signal were observed. Upon addition of Hg^{2+}, the Y-DNA structure was transformed to hairpin structure based on the formation of T-Hg^{2+}-T complex. During the transformation, the redox MB gets close to and the redox Fc gets far away from the electrode surface, respectively. This special design allows a reliable Hg^{2+} detection with a detection range from 1 nM to 5 μM and a low detection limit down to 0.094 nM. Furthermore, this biosensor exhibits good selectivity and repeatability, and can be easily regenerated by using L-cysteine. This study offers a simple and effective method for designing ratiometric biosensors for detecting other ions and biomolecules.

© 2016 Elsevier B.V. All rights reserved.

1. Introduction

Mercury ion (Hg^{2+}) has been widely recognized as one of the most toxic heavy metals due to its accumulative and toxic properties in the environment and mercury-mediated toxicity also has permanent damage to the human central nervous system and other organs [1–4]. To reduce the damage of Hg^{2+} contamination, the US Environmental Protection Agency (EPA) has set the detection limit of Hg^{2+} down to 10 nM in drinking water [5]. Therefore, the exploration of new approaches for detecting Hg^{2+} in disease prevention and environmental protection has attracted intense attention. To date, various analytical techniques for sensing Hg^{2+} have been developed, such as atomic absorption/emission

* Corresponding author.
** Corresponding author.
E-mail addresses: luohq@swu.edu.cn (H.Q. Luo), linb@swu.edu.cn (N.B. Li).

http://dx.doi.org/10.1016/j.aca.2015.12.028
0003-2670/© 2016 Elsevier B.V. All rights reserved.

Please cite this article in press as: J. Jia, et al., A regenerative ratiometric electrochemical biosensor for selective detecting Hg^{2+} based on Y-shaped/hairpin DNA transformation, Analytica Chimica Acta (2016), http://dx.doi.org/10.1016/j.aca.2015.12.028

spectroscopy (AAS/AES) [6,7], inductively coupled plasma-mass spectrometry (ICP-MS) [8], inductively coupled plasma-atomic emission spectrometry (ICP-AES) [9], cold vapor atomic absorption spectroscopy [10], and electrochemiluminescence [11]. Although these methods are very sensitive and selective, creating new strategies with high sensitivity, selectivity and low background interference, and requiring inexpensive instruments as well as simple operation processes still remain a challenge.

Electrochemical biosensor has received much attention for its advantages of high sensitivity, good selectivity, low cost, and simplicity for target detection [12]. It has been widely applied in the detection of meaningful analytes, including specific proteins [13], nucleic acids [14], and small-molecule targets [15]. It has been proved that the thymine–thymine (T–T) mispairs could selectively capture Hg^{2+} to form T-Hg^{2+}-T base pairs, and Hg^{2+}-mediated T-Hg^{2+}-T pair is more stable than the Watson–Crick (WC) A-T pair [16]. By utilizing the strong T-Hg^{2+}-T interaction, many electrochemical biosensors with excellent performance on selectivity have been developed.

Based on the decrease or increase of the signal, the electrochemical biosensors are divided into “signal-off” and “signal-on” subgroups, respectively [17]. In a “signal-off” biosensor, target binding restricts collisions between the redox species and the electrode surface thereby reducing the response signal. This signal-off mechanism suffers the difficulty in adopting signal amplification strategies because the biosensor can never suppress more than 100% of the original signal [18]. In a “signal-on” biosensor, it not only pushes the detected background signal toward zero in the absence of the target, but also employs a lot of signal amplification methods to achieve enormous signal gain without limit in theory [19]. As false positive or negative errors may occur during the process of target detection due to some test-environmental changes, the single-signaling (“signal-off” or “signal-on”) biosensors are subjected to some limitations for practical applications [20]. There is no doubt that the use of dual-signaling response as the signal readout enables the detection method to be relatively reliable and convincing, improving the accuracy of target detection in the complicated environments. Besides the recent advances, almost all of the mechanisms of biosensors were based on “signal-off” or “signal-on” alone. Now a growing number of studies focus on the ratiometric electrochemical sensors due to the advantages of the dual-signaling strategies [20–24], such as diversification of data analysis, good selectivity, high sensitivity, and good repeatability.

Nucleic acids have become a common material in developing novel electrochemical biosensors for their high selectivity in molecular recognition [25]. The most widely used structures of nucleic acids in electrochemical sensing platforms are single-strand and double helical conformations. Furthermore, the abundant secondary structures of nucleic acids such as hairpin [26], G-quadruplex [27], hand-in-hand [28], cruciform [29], and pseudoknot [30] have been widely applied in sensing platforms because of the roles they played in transcription regulatory mechanisms. Among various secondary structures, Y-DNA is composed of three single-strand DNAs (ssDNAs), each of which is partially complementary to the other two ssDNAs and it could be achieved by stepwise as well as all-in-one (one-pot) synthesis methods [31]. Y-DNA can grow to supramolecular nanoarchitectures such as dendrimers with multiple functions as its branch DNA can be designed to contain different functional moieties by designing different branch sequences [32]. The dendrimers are potentially conducive to widespread in vivo applications such as gene and drug delivery, tissue repair, and imaging [33].

Moreover, some efforts have gone into developing the Y-DNA-based biosensors due to the advantages of conformational stability and structural flexibility of Y-DNA. For example, Chen and coworkers reported a Y-shaped probe electrochemical biosensor [34], which is simple, sensitive, and stable, and has excellent discrimination ability for single-base mismatch. His group also provided a novel and simple approach for the genotyping/detection of single-nucleotide polymorphisms (SNPs) in trace salivary DNA of oral cancer based on a Y-shaped probe [35].

In an effort to combine the advantages of dual-signaling strategy and Y-DNA, herein, we demonstrated a novel and simple ratiometric biosensor for Hg^{2+} detection via target-induced transformation between Y-DNA and hairpin DNA. This biosensor is easy to be fabricated without time-consuming operation on the electrode. It also shows high selectivity and good repeatability, and can be easily regenerated by using L-cysteine. Moreover, this study offers a simple and effective method for designing ratiometric biosensors for detecting other ions and biomolecules.

2. Materials and methods

2.1. Chemicals and reagents

L-cysteine (L-cys) and HPLC-purified oligonucleotides were purchased from Sangon Biotechnology Co., Ltd. (Shanghai, China), and their base sequences are as follows: Y1 probe: 5′–SH–$(CH_2)_6$-CTG TTT TCT TTC GGA CGA CCC CCC TCG TCC GTT TGT TTT CAG-MB^+-3′; Y2 probe: 5′-AAA ACA AAA AAG AAA AGC C-Fc-3′. Tris (2-carboxyethyl) phosphine hydrochloride (TCEP), 6-mercaptohexanol (MCH), and ethylenediaminetetraacetic acid (EDTA) were purchased from Sigma Chemical Co. (St. Louis, MO, USA). The buffer solutions are as follows: A-buffer solution was 10 mM TE-10 mM TCEP-1 M NaCl solution (pH 8.0); B-buffer solution was 10 mM TE-1.0 M NaCl solution (pH 8.0); electrochemical measurement buffer solution was 10 mM phosphate buffer (pH 7.4) containing 500 mM NaCl and 2.7 mM KCl; washing buffer solution was 10 mM phosphate buffer containing 0.1 M NaCl (pH 7.4). All solutions were prepared with ultrapure water (specific resistance of 18.2 MΩ cm). $Hg(NO_3)_2$, $Ca(NO_3)_2{\cdot}4H_2O$, $Fe(NO_3)_3$, $ZnCl_2$, $Pb(NO_3)_2$, $Co(NO_3)_2$, $Al(NO_3)_3{\cdot}9H_2O$, $Cd(NO_3)_2{\cdot}4H_2O$, $Cr(NO_3)_3{\cdot}9H_2O$, $Cu(NO_3)_2$, $Ba(NO_3)_2$, $Mg(NO_3)_2{\cdot}6H_2O$, $K_3[Fe(CN)_6]$, $K_4[Fe(CN)_6]$, Na_2HPO_4, and NaH_2PO_4 chemicals were of analytical reagent grade and were used without further purification.

2.2. Apparatus

All electrochemical measurements were monitored on an electrochemical workstation (CHI 660D, CH Instruments, Chenhua Corp, Shanghai, China) at room temperature. The experiment was performed with a typical three electrode system, in which the working electrode was the functionalized gold electrode, the reference electrode was an Ag/AgCl electrode with saturated KCl, and the counter electrode was a platinum electrode.

Ferricyanide solution (5.0 mM $[Fe(CN)_6]^{3-/4-}$) used as the supporting electrolyte medium was obtained by dissolving potassium ferrocyanide and potassium ferricyanide (1:1) with phosphate buffer (0.1 M, pH 7.4). Cyclic voltammetry (CV) was performed within the potential range from −0.3 to 0.7 V at 0.1 V s^{-1}. Electrochemical impedance spectra (EIS) were performed in a frequency range from 0.1 Hz to 10 kHz with 5 mV as the amplitude.

2.3. Electrode pretreatment

The gold electrode (4.0 mm in diameter) was polished carefully with alumina powder (1.0, 0.3, and 0.05 μm in diameter) on a micro cloth pad in sequence until a mirror surface was formed, followed by ultrasonic cleaning with ultrapure water, ethanol, and ultrapure

Please cite this article in press as: J. Jia, et al., A regenerative ratiometric electrochemical biosensor for selective detecting Hg^{2+} based on Y-shaped/hairpin DNA transformation, Analytica Chimica Acta (2016), http://dx.doi.org/10.1016/j.aca.2015.12.028

water for 5 min each to remove the residual Al_2O_3 powder. The above electrode was electrochemically cleaned by cycling the potential between −0.2 and + 1.6 V (vs. Ag/AgCl) at 0.1 V s^{-1} in a 0.5 M H_2SO_4 solution until a steady-state redox wave was obtained. Finally, the prepared electrode was rinsed with ultrapure water and dried with nitrogen.

2.4. Biosensor preparation

Before immobilization on the Au electrode surface, the Y1 and Y2 probes were dissolved in A-buffer and B-buffer, respectively, and stored at 4 °C overnight. A mixture of Y1 and Y2 probe solution was heated at 90 °C for 5 min, followed by slowly cooling down to room temperature over 2 h, and the Y1 and Y2 probes would hybridize to form Y-DNA. The cleaned electrode was immersed in 25 μL of the mixture of Y-DNA solution for different time at room temperature to obtain the Y1−Y2/Au electrode. The Y1−Y2/Au electrode was further immersed into 2 mM MCH solution for 1 h to block the uncovered electrode surface as well as to make the array of Y-DNA on the electrode interface more regular. The obtained electrode is labeled as the MCH/Y1−Y2/Au electrode.

2.5. Detection of Hg^{2+}

For the Hg^{2+} detection, the prepared biosensor was then immersed in 100 μL of Hg^{2+} solution with different concentrations at room temperature for 1.6 h to form T-Hg^{2+}-T complex. Then the electrochemical performance of the biosensor was investigated by square wave voltammetry (SWV) in the electrochemical measurement buffer solution. The control experiments for various metal ions were performed under the same conditions. After the detection of Hg^{2+}, the biosensor was regenerated by immersing the electrode into 1 mM L-cysteine solution for 1 h and 3 μM Y2 probe solution for 5 h in sequence. After being washed with the washing buffer, the regenerated electrode was reused for another assay.

3. Results and discussion

3.1. Design of the sensing system for Hg^{2+} detection

The experimental principle of the biosensor is illustrated in Scheme 1. The Y1 probe consisted of three parts and labeled at its 5′ distal terminus with a thiol group and 3′ distal terminus with a redox reporter methylene blue (MB). In three regions: region II is a "stem-loop" structure designed with 7 complementary base pairs in stem region and 6C bases in loop, region I is the part near the 5′ distal terminus and region III is the part near the 3′ distal terminus. Regions I and III contain 7 pairs of T bases and could form T-Hg^{2+}-T complexes in the presence of Hg^{2+}. The Y2 probe modified with a redox tag ferrocene (Fc) at 3'-terminal is complementary to regions I and III of Y1 probe. As demonstrated in a previous study [31], the Y1 and Y2 probes would hybridize to form Y- DNA in the process of annealing.

Since the Y1 probe is dually labeled with 5′-SH and 3′-MB, the Y-DNA can self-assemble on the electrode surface through Au−S bond. When the self-assembling of Y-DNA on the electrode is succeeded, the Y-DNA structure made the MB relatively far from the electrode surface and Fc close to the electrode surface. As a result, the peak current of MB was small and that of Fc was obvious. With the addition of Hg^{2+}, the Y-DNA structure was transformed to hairpin structure according to Scheme 1 by the formation of T-Hg^{2+}-T. This transformation results in the getting close of MB tags to the electrode surface and the dissociating of Y2 probes from the electrode surface. As a result, the current signal of MB increased significantly, which realized signal-on strategy, while the current signal of Fc significantly decreased, which realized signal-off strategy. The dual-current signal ratiometric strategy improved the precision and sensitivity of the measurement. Furthermore, it has been reported in the literature that the binding constant between Hg^{2+} and T:T mismatched base pair in the DNA is nearly 4.14×10^6 L mol^{-1}, while the binding constant between Hg^{2+} and L-cysteine is about 1.26×10^{10} L mol^{-1}. The binding between L-cysteine and Hg^{2+} is so strong that T−Hg^{2+}−T complexes are destroyed and thus Hg^{2+} is removed [12,36]. Therefore, upon the addition of L-cysteine, the Hg^{2+} would bond to L-cysteine effectively and thus induce the release of regions I and III of Y1 probe that

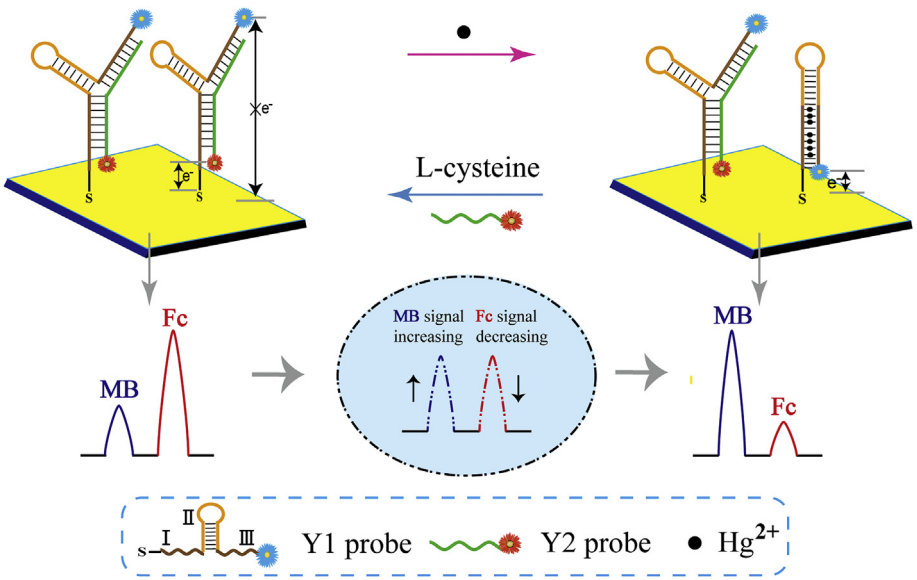

Scheme 1. Schematic illustration of the regenerative ratiometric electrochemical biosensor for selective detection of Hg^{2+} based on Y-shaped/hairpin DNA transformation.

Please cite this article in press as: J. Jia, et al., A regenerative ratiometric electrochemical biosensor for selective detecting Hg^{2+} based on Y-shaped/hairpin DNA transformation, Analytica Chimica Acta (2016), http://dx.doi.org/10.1016/j.aca.2015.12.028

could hybridize with Y2 probe to form Y-DNA again [37]. Consequently, a regenerative ratiometric biosensor used to detect Hg^{2+} was developed based on Y-DNA.

3.2. Feasibility of the biosensor

To demonstrate the feasibility of the Y-DNA-based biosensor, SWV responses of the differently modified electrodes were investigated to verify the construction process of the biosensor. As shown in Fig. 1, the MCH/Y1−Y2/Au electrode has a weak peak current of MB at about −0.28 V and a large peak current of Fc at about 0.40 V (curve a), indicating that the Y-DNA had been formed perfectly by hybridization of Y1 probe with Y2 probe and was assembled on the electrode surface successfully. When the MCH/Y1−Y2/Au electrode was incubated in 10 mM phosphate buffer without Hg^{2+} for 1.6 h, no obvious changes of the current signals of MB and Fc were observed (curve b). However, when the MCH/Y1−Y2/Au electrode was further incubated in the Hg^{2+} solution (5 μM) for 1.6 h, the peak current of MB increased, whereas the peak current of Fc decreased obviously (curve c). These phenomena maybe result from the successful construction of the DNA double-helix structure between regions I and III of Y1 probe due to the formation of T-Hg^{2+}-T. This conformation change leads to the getting close of MB tags to the electrode surface and the getting away of Y2 probe with the Fc tag from the electrode surface. Then, when the above electrode was further incubated in 1.0 mM L-cysteine solution, the peak current of MB decreased and that of Fc had no obvious change (curve d). This is because Hg^{2+} would bond to L-cysteine effectively and then induce region III of Y1 probe to unfold (flexible and dynamic). In this case, the MB tag was not as close to the electrode surface as the situation when the Hg^{2+} existed. After the electrode was incubated with 3 μM Y2 probe solution, the peak current of MB decreased whereas Fc peak current increased (curve e), and both MB and Fc current signals almost retained their original values (curve e vs curve a). This is because Y2 probe was hybridized with Y1 probe to reform Y-DNA on the electrode surface. These results clearly indicated that the developed dual-signaling biosensor was successfully constructed and could be regenerated effectively.

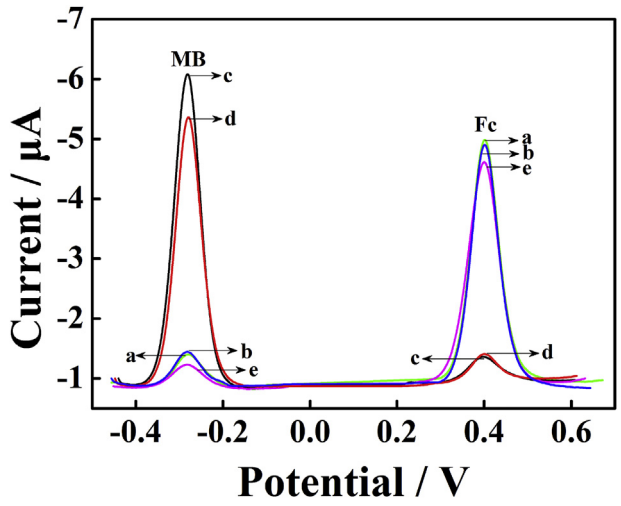

Fig. 1. Square wave voltammograms of different electrodes: MCH/Y1−Y2/Au (a), MCH/Y1−Y2/Au incubated with 100 μL of 10 mM phosphate buffer (0 μM Hg^{2+}) for 1.6 h (b), MCH/Y1−Y2/Au incubated with 100 μL of Hg^{2+} solution (5 μM) for 1.6 h (c), electrode of (c) incubated with 25 μL of L-cysteine solution (1.0 mM) for 1 h (d), and electrode of (d) incubated with 25 μL of Y2 probe solution (3 μM) for 5 h (e). Data were obtained in 10 mM phosphate buffer (pH 7.4) containing 500 mM NaCl and 2.7 mM KCl and the potential range is from −0.45 to 0.65 V.

3.3. Characterization of assembly on the electrode

CV is an effective tool for characterizing the fabrication process and the reaction with the analytes of the electrochemical biosensor. Fig. 2A shows the CV of variously modified electrodes of each step. As shown in Fig. 2A, the peak current of the MCH/Y1−Y2/Au electrode (curve b) decreases and the peak-to-peak separation increases obviously compared to that of the bare electrode (curve a), testifying that the MCH/Y1−Y2 was immobilized successfully on the electrode surface. The peak current increases significantly in the presence of Hg^{2+} (curve c). This is because the T bases of Y1 probe have interacted with the Hg^{2+}, inducing the Y1 probe to form hairpin structure based on T-Hg^{2+}-T complexes and Y2 probe to dissociate away from the electrode surface. Upon the introduction of L-cysteine, the peak current decreases (curve d) for the reason that the Hg^{2+} reacted with L-cysteine and region III of Y1 probe was unfolded. After the addition of Y2 probe, the peak current decreased obviously (curve e), implying that the Y-DNA was successfully formed again on the electrode surface. The above results coincide with the presumptive mechanism of the proposed biosensor.

In the Nyquist plot of EIS, the diameter of the semicircle portion corresponds to the interfacial electron transfer resistance (R_{ct}). The equivalent circuit (inset, Fig. 2B) was used to fit the EIS data which includes the solution resistance (R_s), the constant phase element (CPE) related to double layer capacitance, charge transfer resistance (R_{ct}), and the Warburg impedance (Z_w). Fig. 2B shows the EIS of the electrode in different modification steps, as shown in curve a, the bare electrode shows a tiny semicircle domain (73.4 Ω), indicating a rapid electron transfer process of $[Fe(CN)_6]^{3-/4-}$. After immobilization of the Y1−Y2 complex and MCH, R_{ct} increased (5670.0 Ω, curve b). This is due to the obstruction of the interfacial electron transfer caused by the negatively charged phosphate backbone of Y-DNA and the formation of compact monolayer by MCH. However, the R_{ct} decreased largely (3843.0 Ω, curve c) with addition of Hg^{2+} due to the dissociation of Y2 probe from the electrode surface. The increase in R_{ct} was accompanied with the stepwise modification of L-cysteine (4229.0 Ω, curve d) and Y2 (5545.0 Ω, curve e) on the electrode surface in sequence. The EIS results coincided with the observations of the CV experiments, which further demonstrated that the Y-DNA biosensor has been fabricated successfully.

3.4. Sensitivity of the biosensor

Fig. 3 shows the electrochemical detection of Hg^{2+} based on the proposed Y-DNA biosensor under optimum conditions (see Supplementary data for details, Fig. S1). As shown in Fig. 3A, it is noted that the peak current of MB increases and that of Fc decreases with increasing concentration of Hg^{2+}. The calibration plots of the developed biosensor using individual MB or Fc current signal for Hg^{2+} detection are shown in Fig. 3B, and both of them exhibit good linear logarithmic relationship between the peak current and the concentration of Hg^{2+} in the range of 1 nM−5 μM with detection limits of 0.68 nM and 0.76 nM (S/N = 3), respectively. The inset in Fig. 3B shows the calibration plot of the electrochemical ratiometric assay of Hg^{2+} using I_{MB}/I_{Fc} as the signal. The logarithmic value of I_{MB}/I_{Fc} linearly depends on the logarithm of Hg^{2+} concentration in the range of 1 nM−5 μM with the linear equation $\lg(I_{MB}/I_{Fc}) = 0.5737 \lg C_{Hg}^{2+} - 0.9076$ (R = 0.9953). The detection limit is 0.094 nM (S/N = 3), such a detection limit is much lower than the US EPA standard (10 nM of Hg^{2+} for drinkable water). It is clear that the detection limit value obtained by using I_{MB}/I_{Fc} as the response signal is much lower than that obtained by using I_{MB} or I_{Fc} as the

Please cite this article in press as: J. Jia, et al., A regenerative ratiometric electrochemical biosensor for selective detecting Hg^{2+} based on Y-shaped/hairpin DNA transformation, Analytica Chimica Acta (2016), http://dx.doi.org/10.1016/j.aca.2015.12.028

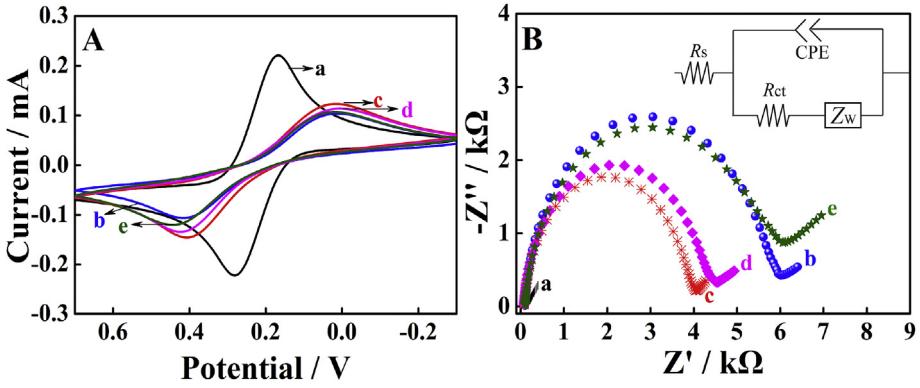

Fig. 2. (A) Cyclic voltammograms and (B) Nyquist diagrams of the biosensor at different stages: bare Au (a), MCH/Y1−Y2/Au (b), MCH/Y1−Y2/Au in the presence of 5 μM Hg^{2+} (c), electrode of (c) incubated in 1.0 mM L-cysteine solution (d), and electrode of (d) incubated in 3 μM Y2 solution (e). Data were obtained in phosphate buffer (0.1 M, pH 7.4) containing 5 mM $[Fe(CN)_6]^{4-/3-}$. The potential range of CV is from −0.3 to 0.7 V at 0.1 V s^{-1} and the frequency range of EIS is 0.1 Hz−10 kHz with 5 mV as the amplitude.

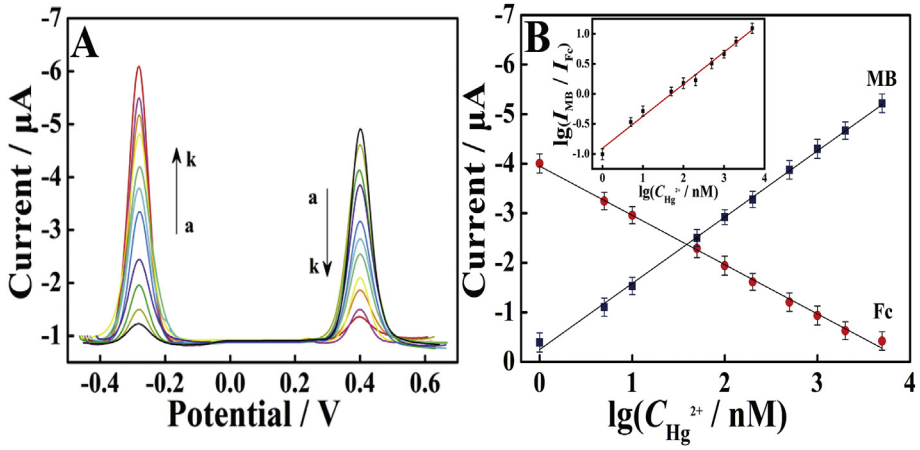

Fig. 3. (A) Square wave voltammograms for the biosensor immersed in different concentrations of Hg^{2+} (a–k): (a) blank (0 nM), (b) 1 nM, (c) 5 nM, (d) 10 nM, (e) 50 nM, (f) 100 nM, (g) 200 nM, (h) 500 nM, (i) 1 μM, (j) 2 μM, and (k) 5 μM. Inset: logarithmic dependence of I_{MB}/I_{Fc} on Hg^{2+} concentration. (B) The linear fit plots of the MB and Fc peak currents as a function of the logarithm of Hg^{2+} concentration. Error bars represent the standard deviation of three parallel experiments. The experimental conditions are the same as that in Fig. 1.

response signal. This result is comparable to or better than those of most existing methods (Table S1). Moreover, unlike the electrochemical biosensors formed by ssDNAs, their DNA hybridization processes which were completed on the electrode surfaces needed a much longer time and more cumbersome operation steps [38,39], the Y-DNA of our biosensor can be easily formed in the process of annealing and has good conformational stability. Thus, not only a great deal of time was saved, but also the preparation procedure of biosensor was simplified when Y-DNA, instead of ssDNA, was assembled on the electrode surface.

3.5. Selectivity, stability and repeatability of the biosensor

Besides the detection sensitivity, the selectivity of a sensing system is another critical factor to evaluate the capability of a biosensor. To investigate the selectivity of the proposed biosensor, a series of commonly existing metal ions including Cu^{2+}, Al^{3+}, Co^{2+}, Fe^{3+}, Zn^{2+}, Ni^{2+}, Cd^{2+}, Ba^{2+}, Cr^{3+}, Mg^{2+}, and Pb^{2+} were studied under optimum conditions with the same experimental procedures in this work (Fig. 4A). When 100 μM those typical metal ions were incubated, respectively, the I_{MB}/I_{Fc} signals were almost the same as that of the background. However, the I_{MB}/I_{Fc} signal of the biosensor in the presence of Hg^{2+} is tremendously higher than that in the presence of other metal ions. Moreover, the response signal of the proposed dual-signaling biosensor is much lower than that of single-signaling biosensor (signal-on) in the presence of the typical metal ions (Fig. 4B). These clearly indicate that the proposed biosensor possesses an excellent selectivity for Hg^{2+} against other environmentally relevant metal ions. Furthermore, the MCH/Y1−Y2/Au electrode was stored in the refrigerator at 4 °C for 10 days and the current signals of the biosensor had no obvious changes (Fig. S2), indicating that the developed electrochemical biosensor has a satisfactory stability.

The repeatability of the proposed biosensor was also investigated by using five equally prepared electrodes to detect Hg^{2+} (1 nM) under same conditions. Five electrodes exhibited similar current responses and a relative standard deviation (RSD) was 3.62%. This is due to the advantage of self-calibration of the dual-signaling strategy, the I_{MB}/I_{Fc} signal is not easy to be interfered by small changes in test environment. The results manifested that the proposed biosensor has satisfactory repeatability.

3.6. Regeneration of biosensor

The regeneration of a biosensor is an important factor for practical application. Here, L-cysteine was employed to remove Hg^{2+} from the T-Hg^{2+}-T complexes. After the reaction with Hg^{2+}, the biosensor was immersed in L-cysteine solution for 1 h at room

Please cite this article in press as: J. Jia, et al., A regenerative ratiometric electrochemical biosensor for selective detecting Hg^{2+} based on Y-shaped/hairpin DNA transformation, Analytica Chimica Acta (2016), http://dx.doi.org/10.1016/j.aca.2015.12.028

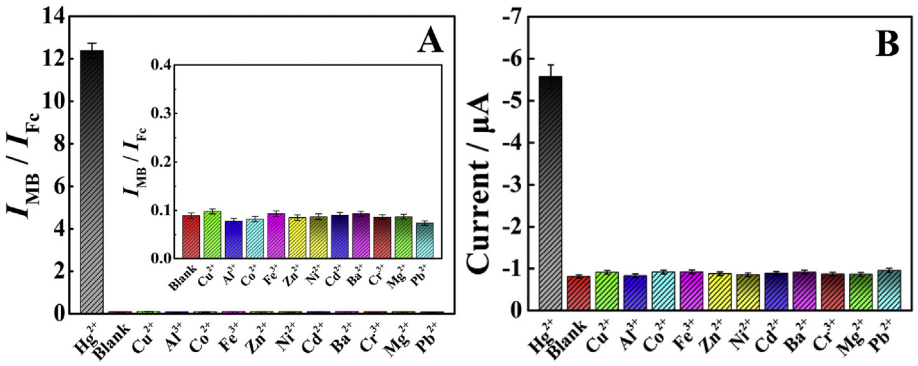

Fig. 4. Selectivity of the ratiometric biosensor (A) and signal-on biosensor (B) for Hg^{2+} detection. The concentration of all interfering metal ions was 100 μM, and that of Hg^{2+} was 5 μM. The experimental conditions are the same as that in Fig. 1. Error bars represent the standard deviation of three replicates from one electrode.

temperature. The Hg^{2+} would bond to L-cysteine effectively and induce regions I and III of Y1 probe to be free so as to be hybridized with Y2 probe to reform Y-DNA on the electrode surface again. Fig. 5 shows the current signals of the Y-DNA biosensor immersed alternately in the solutions of 5.0 μM Hg^{2+}, 1.0 mM L-cysteine, and 3.0 μM Y2 probe for five regeneration cycles. It can be seen that the current signals changed reversibly, and both MB and Fc current signals almost retained their original values after five cycles. It is consistent with the literature that the L-cysteine does not affect the response and repeatability of the biosensor [40]. In conclusion, the developed dual-signaling biosensor can be readily regenerated.

3.7. Practical application

To evaluate whether this biosensor is applicable to natural samples, this biosensor was used to detect Hg^{2+} in water samples from Jialing River. Prior to use, the samples collected were filtered by 0.2 μm membranes to remove impurities. The experimental result indicated that the Hg^{2+} was not found in the water samples. Moreover, the water samples spiked with Hg^{2+} at three different concentrations of 1, 100, and 5000 nM were tested. The results are listed in Table S2 and the recovery of Hg^{2+} in the range of 96.8–107.6% was achieved, which demonstrated the feasibility of this method in real samples.

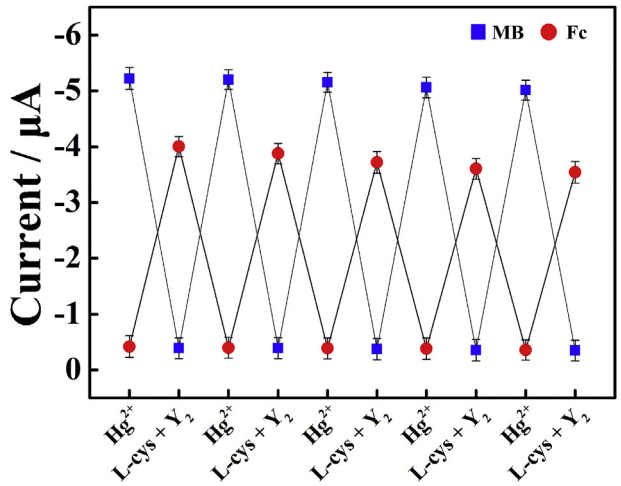

Fig. 5. Reversible changes of the MB and Fc peak currents for the biosensor immersed in the solution of 5 μM Hg^{2+}, 1.0 mM L-cysteine, and 3 μM Y2 probe, alternately. The experimental conditions are the same as that in Fig. 1. Error bars represent the standard deviation of three replicates from one electrode.

4. Conclusions

This work proposed a facile and sensitive ratiometric biosensor for Hg^{2+} detection by using the Y-shaped DNA. The hybridization of two probes with different redox-species labeled in solution formed a Y-shaped DNA, which was assembled on the electrode surface and generated measurable ratiometric electrochemical signal. This dual-signaling biosensor is easy to be fabricated without cumbersome operations on the electrode. What's more, this biosensor with good selectivity and repeatability can be easily regenerated by using L-cysteine. In spite of these merits, our design lacks the signal amplification procedure and should be further improved in the following study.

Acknowledgments

This work was financially supported by the National Natural Science Foundation of China (No. 21273174) and the Municipal Natural Science Foundation of Chongqing City (No. CSTC–2013jjB00002).

Appendix A. Supplementary data

Supplementary data related to this article can be found at http://dx.doi.org/10.1016/j.aca.2015.12.028.

References

[1] P.B. Tchounwou, W.K. Ayensu, N. Ninashvili, D. Sutton, Environmental exposure to mercury and its toxicopathologic implications for public health, Inc. Environ. Toxicol. 18 (2003) 149–175.
[2] M. Gochfeld, Cases of mercury exposure, bioavailability, and absorption, Ecotoxicol. Environ. Saf. 56 (2003) 174–179.
[3] F. Zahir, S.J. Rizwi, S.K. Haq, R.H. Khan, Low dose mercury toxicity and human health, Environ. Toxicol. Pharmacol. 20 (2005) 351–360.
[4] L. Magos, T.W. Clarkson, Overview of the clinical toxicity of mercury, Ann. Clin. Biochem. 43 (2006) 257–268.
[5] D.M. Chen, Z.F. Gao, J. Jia, N.B. Li, H.Q. Luo, A sensitive and selective electrochemical biosensor for detection of mercury(II) ions based on nicking endonuclease-assisted signal amplification, Sens. Actuat. B 210 (2015) 290–296.
[6] J.T. Madden, N. Fitzgerald, Investigation of ultraviolet photolysis vapor generation with in-atomizer trapping graphite furnace atomic absorption spectrometry for the determination of mercury, Spectrochim. Acta Part B 64 (2009) 925–927.
[7] X.P. Zhu, S.D. Alexandratos, Determination of trace levels of mercury in aqueous solutions by inductively coupled plasma atomic emission spectrometry: elimination of the 'memory effect', Microchem. J. 86 (2007) 37–41.
[8] D. Malinovsky, R.E. Sturgeon, L. Yang, Anion-exchange chromatographic separation of Hg for isotope ratio measurements by multicollector ICPMS, Anal. Chem. 80 (2008) 2548–2555.
[9] F.X. Han, W.D. Patterson, Y.J. Xia, B.B.M. Sridhar, Y. Su, Rapid determination of mercury in plant and soil samples using inductively coupled plasma atomic

emission spectroscopy, a comparative study, Water Air. Soil. Pollut. 170 (2006) 161–171.
[10] M.J.d. Silva, A.P.S. Paim, M.F. Pimentel, M.L. Cervera, M.d.l. Guardia, Determination of mercury in rice by cold vapor atomic fluorescence spectrometry after microwave-assisted digestion, Anal. Chim. Acta 667 (2010) 43–48.
[11] Q. Li, X.M. Zhou, D. Xing, Rapid and highly sensitive detection of mercury ion (Hg^{2+}) by magnetic beads-based electrochemiluminescence assay, Biosens. Bioelectron. 26 (2010) 859–862.
[12] E.H. Xiong, L. Wu, J.W. Zhou, P. Yu, X.H. Zhang, J.H. Chen, A ratiometric electrochemical biosensor for sensitive detection of Hg^{2+} based on thymine-Hg^{2+}-thymine structure, Anal. Chim. Acta 853 (2015) 242–248.
[13] J.R. Chen, X.X. Jiao, H.Q. Luo, N.B. Li, Probe-label-free electrochemical aptasensor based on methylene blue-anchored graphene oxide amplification, J. Mater. Chem. B 1 (2013) 861–864.
[14] Q.W. Xue, Y.Q. Lv, H. Cui, X.H. Gu, S.Q. Zhang, J.F. Liu, A DNA nanomachine based on rolling circle amplification-bridged two-stage exonuclease III-assisted recycling strategy for label-free multi-amplified biosensing of nucleic acid, Anal. Chim. Acta 856 (2015) 103–109.
[15] X.L. Chai, L.M. Zhang, Y. Tian, Ratiometric electrochemical sensor for selective monitoring of cadmium ions using ions molecular recognition, Anal. Chem. 86 (2014) 10668–10673.
[16] Y. Miyake, H. Togashi, M. Tashiro, H. Yamaguchi, S. Oda, M. Kudo, Y. Tanaka, Y. Kondo, R. Sawa, T. Fujimoto, T. Machinami, A. Ono, MercuryII-mediated formation of thymine-HgII-thymine base pairs in DNA duplexes, J. Am. Chem. Soc. 128 (2006) 2172–2173.
[17] F.L. Gao, Y. Qian, L. Zhang, S.Z. Dai, Y.F. Lan, Y. Zhang, L.L. Du, D.Q. Tang, Target catalyzed hairpin assembly for constructing a ratiometric electrochemical aptasensor, Biosens. Bioelectron. 71 (2015) 158–163.
[18] Z.G. Yu, R.Y. Lai, A reagentless and reusable electrochemical DNA sensor based on target hybridization-induced stem-loop probe formation, Chem. Commun. 48 (2012) 10523–10525.
[19] X.L. Zuo, Y. Xiao, K.W. Plaxco, High specificity, electrochemical sandwich assays based on single aptamer sequences and suitable for the direct detection of small-molecule targets in blood and other complex matrices, J. Am. Chem. Soc. 131 (2009) 6944–6945.
[20] J.J. Deng, P. Yu, Y.X. Wang, L.Q. Mao, Real-time ratiometric fluorescent assay for alkaline phosphatase activity with stimulus responsive infinite coordination polymer nanoparticles, Anal. Chem. 87 (2015) 3080–3086.
[21] L. Wu, X.H. Zhang, W. Liu, E.H. Xiong, J.H. Chen, Sensitive electrochemical aptasensor by coupling "signal-on" and "signal-off" strategies, Anal. Chem. 85 (2013) 8397–8402.
[22] G.B. Zhu, L. Wu, X. Zhang, W. Liu, X.H. Zhang, J.H. Chen, A new dual-signaling electrochemical sensing strategy based on competitive host–guest interaction of a,b-cyclodextrin/poly(nacetylaniline)/graphene-modified electrode: sensitive electrochemical determination of organic pollutants, Chem. Eur. J. 19 (2013) 6368–6373.
[23] K.W. Ren, J. Wu, F. Yan, H.X. Ju, Ratiometric electrochemical proximity assay for sensitive one-step protein detection, Sci. Rep. 4 (2014) 4360.
[24] K.W. Ren, J. Wu, F. Yan, Y. Zhang, H.X. Ju, Immunoreaction-triggered DNA assembly for one-step sensitive ratiometric electrochemical biosensing of protein biomarker, Biosens. Bioelectron. 66 (2015) 345–349.
[25] P.L. He, L. Shen, Y.H. Cao, D.F. Li, Ultrasensitive electrochemical detection of proteins by amplification of aptamer-nanoparticle bio bar codes, Anal. Chem. 79 (2007) 8024–8029.
[26] X.F. Wei, W.L. Lin, N. Ma, F. Luo, Z.Y. Lin, L.H. Guo, B. Qiu, G.N. Chen, Sensitive fluorescence biosensor for folate receptor based on terminal protection of small-molecule-linked DNA, Chem. Commun. 48 (2012) 6184–6186.
[27] S.M. Haider, G.N. Parkinson, S. Neidle, Structure of a G-quadruplex-ligand complex, J. Mol. Biol. 326 (2003) 117–125.
[28] C. Li, Z.Y. Wang, T. Gao, A.P. Duan, G.X. Li, Fabrication of hand-in-hand nanostructure for one-step protein detection, Chem. Commun. 49 (2013) 3760–3762.
[29] H. Kurahashi, H. Inagaki, K. Yamada, T. Ohye, M. Taniguchi, B.S. Emanuel, T. Toda, Cruciform DNA structure underlies the etiology for palindrome-mediated human chromosomal translocations, J. Biol. Chem. 279 (2004) 35377–35383.
[30] K.A. Afonin1, Y.P. Lin, E.R. Calkins1, L. Jaeger, Attenuation of loop-receptor interactions with pseudoknot formation, Nucl. Acids Res. 40 (2012) 2168–2180.
[31] E.J. Cheng, Y.Z. Xing, P. Chen, Y. Yang, Y.W. Sun, D.J. Zhou, L.J. Xu, Q.H. Fan, D.S. Liu, A pH-triggered, fast-responding DNA hydrogel, Angew. Chem. 121 (2009) 7796–7799.
[32] Y.H. Roh, R.C.H. Ruiz, S.M. Peng, J.B. Lee, D. Luo, Engineering DNA-based functional materials, Chem. Soc. Rev. 40 (2011) 5730–5744.
[33] S. Chatterjee, J.B. Lee, N.V. Valappil, D. Luo, V.M. Menon, Probing Y-shaped DNA structure with time-resolved FRET, Nanoscale 4 (2012) 1568–1571.
[34] J. Zhang, J.H. Chen, R.C. Chen, G.N. Chen, F.F. Fu, Sequence-specific detection of trace DNA via a junction-probe electrochemical sensor employed template-enhanced hybridization strategy, Biosens. Bioelectron. 25 (2009) 815–819.
[35] J. Zhang, X.Y. Wu, P.P. Chen, N.T. Lin, J.H. Chen, G.N. Chen, F.F. Fu, Electrochemical genotyping and detection of single-nucleotide polymorphisms based on junction-probe containing 2′-deoxyinosine, Chem. Commun. 46 (2010) 6986–6988.
[36] F. Chai, C.G. Wang, T.T. Wang, Z.F. Ma, Z.M. Su, L-cysteine functionalized gold nanoparticles for the colorimetric detection of Hg^{2+} induced by ultraviolet light, Nanotechnology 21 (2010) 025501.
[37] Y.Q. Zhang, L.J. Gao, L.P. Wen, L.P. Heng, Y.L. Song, Highly sensitive, selective and reusable mercury(II) ion sensor based on a ssDNA-functionalized photonic crystal film, Phys. Chem. Chem. Phys. 15 (2013) 11943–11949.
[38] D.H. Wu, Q. Zhang, X. Chu, H.B. Wang, G.L. Shen, R.Q. Yu, Ultrasensitive electrochemical sensor for mercury (II) based on target-induced structure-switching DNA, Biosens. Bioelectron. 25 (2010) 1025–1031.
[39] Z.Z. Lin, X.H. Li, H.-B. Kraatz, Impedimetric immobilized DNA-based sensor for simultaneous detection of Pb^{2+}, Ag^{+}, and Hg^{2+}, Anal. Chem. 83 (2011) 6896–6901.
[40] D. Han, Y.-R. Kim, J.-W. Oh, T.H. Kim, R.K. Mahajan, J.S. Kim, H. Kim, A regenerative electrochemical sensor based on oligonucleotide for the elective determination of mercury(II), Analyst 134 (2009) 1857–1862.

Please cite this article in press as: J. Jia, et al., A regenerative ratiometric electrochemical biosensor for selective detecting Hg^{2+} based on Y-shaped/hairpin DNA transformation, Analytica Chimica Acta (2016), http://dx.doi.org/10.1016/j.aca.2015.12.028